Occurrence of nudicaulin structural variants in flowers of papaveraceous species

Evangelos C. Tatsis [a], Hartmut Böhm [b], Bernd Schneider [a,*]

[a] Max Planck Institute for Chemical Ecology, Hans-Knöll-Straße 8, Beutenberg Campus, D-07745 Jena, Germany
[b] Friedrich-Wilhelm-Murnau-Straße 20, D-14480 Potsdam, Germany

ARTICLE INFO

ABSTRACT

The intense color of yellow *Papaver nudicaule* flowers is conferred by the presence of nudicaulins, a group of alkaloids with a unique pentacyclic skeleton composed of an indole ring and a polyphenolic moiety. Petals from eight different Papaveraceae species composed of different color varieties were probed for the presence of nudicaulins. In addition to their occurrence in yellow *P. nudicaule* flowers, nudicaulins **I–VIII** were detected and quantified in orange flowers of *P. nudicaule*, and in yellow and orange *Papaver alpinum* flowers. *Meconopsis cambrica* petals showed a divergent nudicaulin spectrum, with compounds having an attached 3-hydroxy-3-methyl-glutaryl group (HMG) instead of a malonyl unit at one of the glucose units. Flavonols and anthocyanins that accompany nudicaulins were identified. The taxonomical significance of the occurrence of nudicaulins is briefly discussed.

1. Introduction

Both the shape and the color of flowers, especially of petals, play a crucial role in how plants interact with their environment, specifically, in the chemical communication between plants and their pollinators. The color of petals usually is conferred by the presence of distinct chemical structures. Two major classes of flower pigments, anthocyanins and carotenoids, are responsible for the intense colors of most plants' flowers, while pigments such as betalains and aurones are restricted to a limited number of taxonomical units (Grotewold, 2006; Tanaka et al., 2008).

Nudicaulins, an elusive group of flower pigments, generate the color of the dark yellow petals of *Papaver nudicaule*. They were isolated for the first time by Price et al. (1939). Early trials to elucidate their structures led to the conclusion that nudicaulins did not belong to one of the known classes of flower pigments but seemed to be a new group of nitrogen-containing compounds (Harborne, 1965). Based on nuclear magnetic resonance (NMR) spectroscopic and mass spectrometric (MS) analyses, a pentacyclic indole alkaloid skeleton, decorated with a glucose and a sophorose unit, was proposed (Schliemann et al., 2006). Additional NMR experiments and chemical modifications resulted in a revised constitution of the nudicaulin aglycon, namely 12-(4-hydroxyphenyl)-3,

11-dihydrobenzofuro[2′,3′:1]cyclopenta[1,2-*b*]indole-5,7,11-triol (Tatsis et al., 2013). Furthermore, the relative configuration of the two diastereomers, nudicaulin **I** and **II**, was substantiated by rotating-frame Overhauser effect spectroscopy (ROESY) and quantum-chemical calculations, and the absolute configuration was assigned by comparing the results of quantum-chemical circular-dichroism (CD) calculations and experimental CD spectra. From these data, nudicaulin **I** was assigned as the (3*S*,11*R*)-diastereomer and nudicaulin **II** as the (3*R*,11*S*)-diastereomer (Fig. 1), i.e. H-3 and glucose A are oriented to the same side of the aglycon skeleton (*cis* conformation) in each of the diastereomers. While the constitution of the aglycon and the carbohydrate units is not subject to variation in the nudicaulins known so far, acyl units attached to the sugars are the reason for some of the structural diversity of *P. nudicaule*'s typical flower pigments.

In the present study, the petals of four *P. nudicaule* color varieties, three *Papaver alpinum* color varieties, and six other Papaveraceae species were examined for the occurrence of nudicaulins; the structure of the nudicaulins discovered was elucidated.

2. Results

2.1. Identification of compounds

Papaveraceous plants were chosen according to taxonomical relationships, petal colors, and the availability of herbal material

* Corresponding author. Tel.: +49 3641 571600; fax: +49 3641 571601.
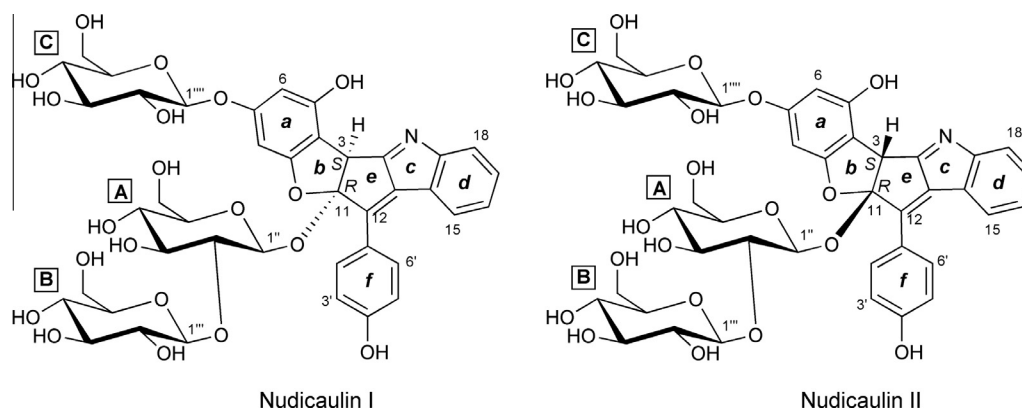E-mail address: schneider@ice.mpg.de (B. Schneider).

Fig. 1. Structures of nudicaulins **I** and **II** (Tatsis et al., 2013).

or seeds. The analyzed plant species and varieties are listed in Table 1. The flavonoids and nudicaulins found in dark yellow petals of *P. nudicaule* were investigated in detail for their structures (Schliemann et al., 2006; Tatsis et al., 2013) and the present studies of respective plant parts follow the reported methods, briefly described in the experimental section. UV/VIS, NMR and MS data confirm a previous report, in which eight nudicaulins (nudicaulin **I**–**VIII**) and the eight flavonols (gossypitrin (**6**), kaempferol 3-*O*-β-sophoroside (**7**) and its isomer (**8**), kaempferol 3-*O*-β-sophoroside-7-*O*-β-glucoside (**1**), kaempferol 3-*O*-β-(sophoroside)-7-*O*-β-[(6-malonyl)glucoside] (**4**), kaempferol 3-*O*-β-[(6-malonyl)sophoroside]-7-*O*-β-glucoside (**2**) and kaempferol 3-*O*-β-[(6-malonyl)sophoroside]-7-*O*-β-[(6-malonyl)glucoside] (**5**) and its isomer (**3**)) were identified or partially characterized (Fig. 2; Schliemann et al., 2006). In the extract obtained from the orange petals of *P. nudicaule*, the anthocyanins pelargonidin 3-*O*-β-sophoroside-7-*O*-β-glucoside (**9**), pelargonidin 3-*O*-β-[(6-malonyl)-sophoroside]-7-*O*-β-glucoside (**10**) and pelargonidin 3-*O*-β-[(6-malonyl)-sophoroside]-7-*O*-β-glucoside (**11**)] were found in addition to nudicaulins **I**–**VIII** and flavonols **1**–**8**. White petals from this species contain flavonols **1**–**8**, and red petals are colored by the pelargonidin derivatives, pelargonidin 3-*O*-β-sophoroside-7-*O*-β-glucoside (**9**), pelargonidin 3-*O*-β-sophoroside (**12**) and pelargonidin 3-*O*-β-[(6-malonyl)-sophoroside] (**13**) (Fig. 2) as reported earlier (Cornuz et al., 1981). Nudicaulins were not found in white and red petals. The spectroscopic data (UV/VIS, NMR, MS) of the isolated compounds are in full agreement with the published data.

P. alpinum was selected for the present study because this poppy is a close relative of *P. nudicaule* within the *Papaver* section *Meconella* Spach (Carolan et al., 2006). Like *P. nudicaule*, *P. alpinum* shows yellow and orange petals but no red pigmentation. Fabergé (1943) reported the occurrence of nudicaulin and pelargonidin glycosides for *P. alpinum* petals. Here, these plant parts were extracted, and their metabolites isolated and analyzed according to published protocols (Schliemann et al., 2006). The HPLC, UV, LC–MS and NMR analysis of extracts from yellow petals revealed the presence of nudicaulins **I**–**VIII** and flavonols **1**–**8**. In the extract obtained from orange petals, the anthocyanins pelargonidin 3-*O*-β-sophoroside-7-*O*-β-glucoside (**9**), pelargonidin 3-*O*-β-[(6-malonyl)-sophoroside]-7-*O*-β-glucoside (**10**) and pelargonidin 3-*O*-β-[(6-malonyl)-sophoroside]-7-*O*-β-[(6-malonyl)-glucoside] (**11**) were found, in addition to nudicaulins **I**–**VIII** and flavonols **1**–**8**. From the white petals of *P. alpinum* the flavonols **1**–**6** have been identified.

A number of other *Papaver* species, namely *P. pilosum*, *P. atlanticum*, *P. aculeatum*, *P. californicum* and *P. somniferum*, were selected for the present investigation in light of their different taxonomical relation to a member of the genus *Meconopsis*, *M. cambrica* (Carolan et al., 2006). However, nudicaulins were not found in the petals of all these *Papaver* species. Instead, the color of the petals seems to be dominated by anthocyanins (data not shown). After the lack of nudicaulins was proven unequivocally, the respective experiments were finished.

Price et al. (1939) reported the occurrence of nudicaulins in the yellow flowers of *Meconopsis cambrica*. This was confirmed by chromatographic comparison and UV/VIS spectroscopy with samples from *P. nudicaule* (Böhm, 1984, unpublished). However, the structural details of the nudicaulins in *M. cambrica* are still unknown. Investigation of flower extracts by HPLC analysis at 460 nm, a wavelength characteristic for nudicaulins, revealed the presence of five major peaks (Fig. 3). On the basis of their UV/VIS spectra, retention times, and mass spectra, nudicaulins **I**, **II**, **V** and **VI** have been identified. No HPLC peaks at R_t 19.1 and 19.3 min of molecular ion masses of *m/z* 958 were found, suggesting that the monomalonylated nudicaulins **III** and **IV** do not occur in *M. cambrica*. The same applies to dimalonylated nudicaulins **VII** (R_t 22.0 min, *m/z* 1044) and **VIII** (R_t 22.6 min, *m/z* 1044). Nudicaulins **III** and **IV**, where the malonyl unit is attached to 6-OH of glucose A, and nudicaulins **V** and **VI**, where the malonyl unit is attached to 6-OH of glucose C (Fig. 2), were not only distinguished by their retention times (Fig. 3) but also the MS/MS spectra of their molecular cations (Schliemann et al., 2006).

The absorption maxima at 214, 258, 335, and 458 nm in the UV/VIS spectra of the HPLC peak eluted at 21.2 min suggested the presence of nudicaulin in a *M. cambrica* flower extract (Fig. 3). This chromatographic peak showed a molecular ion mass of *m/z* 1016 and mass fragments at *m/z* 854, 692, and 386. The cation of *m/z* 386 corresponds to the mass of nudicaulin aglycon, while the cations with masses of *m/z* 854 and 692 indicate the loss of one and two glucose units from the molecular cation of *m/z* 1016, respectively. The MS data point to the presence of a nudicaulin derivative, probably one with the same glucosidic moiety as nudicaulins **I**–**VIII**. Given the difference of molecular mass ion *m/z* 1016 with the molecular ion of non-acylated nudicaulins **I** and **II** *m/z* 872, and taking into account the fact that water is eliminated during esterification, the conjugation of an acyl unit with the elemental composition $C_6H_9O_4$ was concluded to have taken place. The fraction eluted at R_t 21.2 was further separated by preparative HPLC and measured by NMR. The ^1H NMR spectrum shows two sets of analogous signals with minor chemical shift differences between them, suggesting the presence of two co-eluting compounds, namely **IX** and **X**, of the nudicaulin type. In the aglycon parts of the nudicaulin molecules, the only major chemical shift difference was observed for the signals of the protons (H-3) attached to the chiral center at C-3, appearing at δ 5.80 and 5.63. Similar chemical shift differences have been observed for diastereomeric pairs of nudicaulins (Schliemann et al., 2006; Tatsis et al., 2013). Therefore it was concluded that compounds **IX** and **X** are diastereomeric counterparts. Since the concentrations of the two co-eluted

Table 1
Occurrence and concentration of nudicaulins in petals of Papaveraceae species.

Species/variety	Flower color	Occurrence of nudicaulins	Nudicaulin **I**	Nudicaulin **II**
			% of DW1	% of DW[a]
P. nudicaule	Yellow	**I–VIII**	1.48	1.17
	Red	nd		
	White	nd		
	Orange	**I–VIII**	1.12	0.83
P. alpinum	Yellow	**I–VIII**	1.02	0.78
	White	nd		
	Orange	**I–VIII**	0.71	0.65
P. pilosum	Pink	nd		
P. atlanticum	Violet	nd		
P. aculeatum	Orange	nd		
P. californicum	Orange	nd		
P. somniferum nigrum	Purple	nd		
P. somniferum album	White	nd		
M. cambrica	Yellow	**I, II, V, VI, IX, X**	1.44	1.17

[a] The crude extracts containing mixtures of non-acylated and acylated nudicaulins were subject to basic hydrolysis to afford a total amount of the non-acylated nudicaulins **I** and **II**. The concentration (% of dry weight; average of three replicates) of the diastereomeric counterparts in the respective hydrolysate was determined by HPLC. DW: dry weight. nd: Not detectable.

diastereomers are not in a one-to-one ratio, the different intensities of the NMR signals were used to distinguish the signals of the two compounds.

The assignment strategy reported by Schliemann et al. (2006) and Tatsis et al. (2013) was applied to the ^{1}H NMR and 2D correlation data (^{1}H–^{1}H COSY, TOCSY, HSQC and HMBC) of the mixture of the diastereomers **IX** and **X**. Briefly, the ^{1}H NMR, ^{1}H–^{1}H COSY and HSQC spectra show the characteristic signals belonging to each of the two aglycons: the AX system of two doublets of H-6 and H-8 (ring **a**), the four-spin system of H-15–H-18 of the 1.2-disubstituted ring **d** of the indole moiety, the AA′XX′ system of H-2′/6′ and H-3′/5′ from the 1,4-substituted ring **f**. In addition, singlets of H-3 were observed, which proved to be critical for establishing the connections between the substructures by means of HMBC correlations. The strong cross-signal in the ROESY spectrum (Fig. S3) between H-15 and H-2′/6′ substantiated the [2′,3′:1]-annelation of the indole moiety to the central cyclopentene ring **e**. According to our results and the previous findings of Tatsis et al. (2013), the spectroscopic data are in agreement with the nudicaulin aglycon structure as 12-(4-hydroxyphenyl)-3,11-dihydrobenzofuro[2′,3′:1]cyclopenta[1,2-*b*] indole-5,7,11-triol.

The attachment of carbohydrate units were established by HMBC correlations of protons at the anomeric centers of glucose C with C-7 and of glucose A with C-11. The HMBC cross-signal between the proton at the anomeric center of glucose B with C-2″ of glucose A indicated the interglucosidic bond between the two glucose units of the sophorose. The deshielded methylene carbons C-6‴ (δ 64.3 and 64.1) and H-6‴A/B (δ 4.44/4.42; δ 4.22/4.20) (Table 2) suggested acyl substitution at this hydroxymethylene group of **IX** and **X**. An HSQC cross-signal at δ_H 1.21/δ_C 27.8 was assignable to a methyl group of **IX** and one at δ_H 1.28/δ_C 27.7 s was assigned to a methyl group of **X** (Fig. S1). The methyl group signals are inconsistent with any known nudicaulin structural features and, therefore, must be attributed to the C$_6$ acyl unit. Each of the methyl signals displayed HMBC cross-peaks (Fig. S2) with the signal of an oxygenated carbon atom (δ 70.8/ δ 70.8) and two methylenes (**IX**: δ 46.4, 45.6; **IX**: δ 46.4, 45.8). In turn, the methylene protons of **IX** (δ 2.53/2.48; δ 2.64/2.57) and **X** (δ 2.62/2.57; δ 2.72/2.66) correlated with the corresponding methyl groups. HMBC correlations through two bonds between the two methylene ^{1}H NMR signals of the acyl units of each diastereomer and a carbonyl carbon signal (**IX**: δ 2.53/2.48 → δ 172.4; δ 2.64/2.57 → δ 174.9; **X**: δ 2.62/2.57 → δ 172.3; δ 2.72/2.66 → 175.0) and the oxygenated carbon atom (δ 70.8/70.8) (Fig. S2) were observed.

These MS and NMR results allowed the acyl-type substituent to be identified as a 3-hydroxy-3-methyl-glutaryl (HMG) group. The attachment of the HMG part to the hydroxymethylene group of glucose C was confirmed by the correlation peak in the HMBC spectrum (Fig. S2), between H-6‴A/B (δ 4.44/4.42; δ 4.22/4.20), and the carbonyl ester carbon of the HMG unit at δ 172.3/172.4. The HMG as an acyl group attached to Glc-6-OH is common for the lignan macromolecule in *Linum* seeds (Struijs et al., 2008), for example, and has been also reported in petal constituents (Morikawa et al., 2009). In light of these data, nudicaulins **IX** and **X** were identified as isomeric 12-(4-hydroxyphenyl)-3,11-dihydrobenzofuro[2′,3′:1]cyclopenta[1,2-*b*]indole-5-hydroxy-7-*O*-β-[6-(3-hydroxy-3-methyl-glutaryl)glucoside]-11-*O*-β-sophoroside.

In the ROESY spectrum (Fig. S3), cross-signals between H-3 and H-1″ of glucose A were observed for both nudicaulin **IX** and **X**, indicating *cis*-configuration, i.e. C(3)-H and C(11)-O-GlcA are oriented to the same side of the aglycon skeleton in each of the diastereomers, as recently reported for nudicaulin **I** and **II** (Tatsis et al., 2013). Moreover, using the integral intensity of the ROESY cross-signals between H-2′/6′ and H-3′/5′ as references (100%), the integral intensity of the H-3–H-1″ cross-signal of nudicaulin **IX** was 55% and that of nudicaulin **X** was 17%. Different intensities of the H-3–H-1″ ROESY cross-signals were also observed for the diastereomeric pair nudicaulin **I** and **II** (Tatsis et al., 2013). From this analogy and with similar NMR data from nudicaulin **IX** and **X** and from nudicaulin **I** and **II**, the absolute configuration for nudicaulin **IX** seemed to be (3*S*,11*R*) and that for nudicaulin **X** (3*R*,11*S*). This suggestion was confirmed by the deacylation of a crude nudicaulin mixture, resulting in nudicaulin **I** and **II** with known absolute configuration (Tatsis et al., 2013).

The only well-resolved signals between the two diastereomers nudicaulin **IX** and **X** were the signals of methyl groups from the HMG moiety, the signals of H-2′/6′ and the signals of H-3. The integration of those signals (Fig. S4) revealed a ratio of 1.2:1 in each case between nudicaulin **IX** and nudicaulin **X**, indicating that the two diastereomers are present in a scalemic mixture.

2.2. Quantification of nudicaulins

Eight of ten nudicaulins, which have been identified in flowers of Papaveraceae, exist in the form of acylated glucosides. In order to compare total nudicaulin concentrations of the studied species and varieties, the acyl units were removed by basic hydrolysis. As a result of hydrolysis, the compound pattern was simplified to
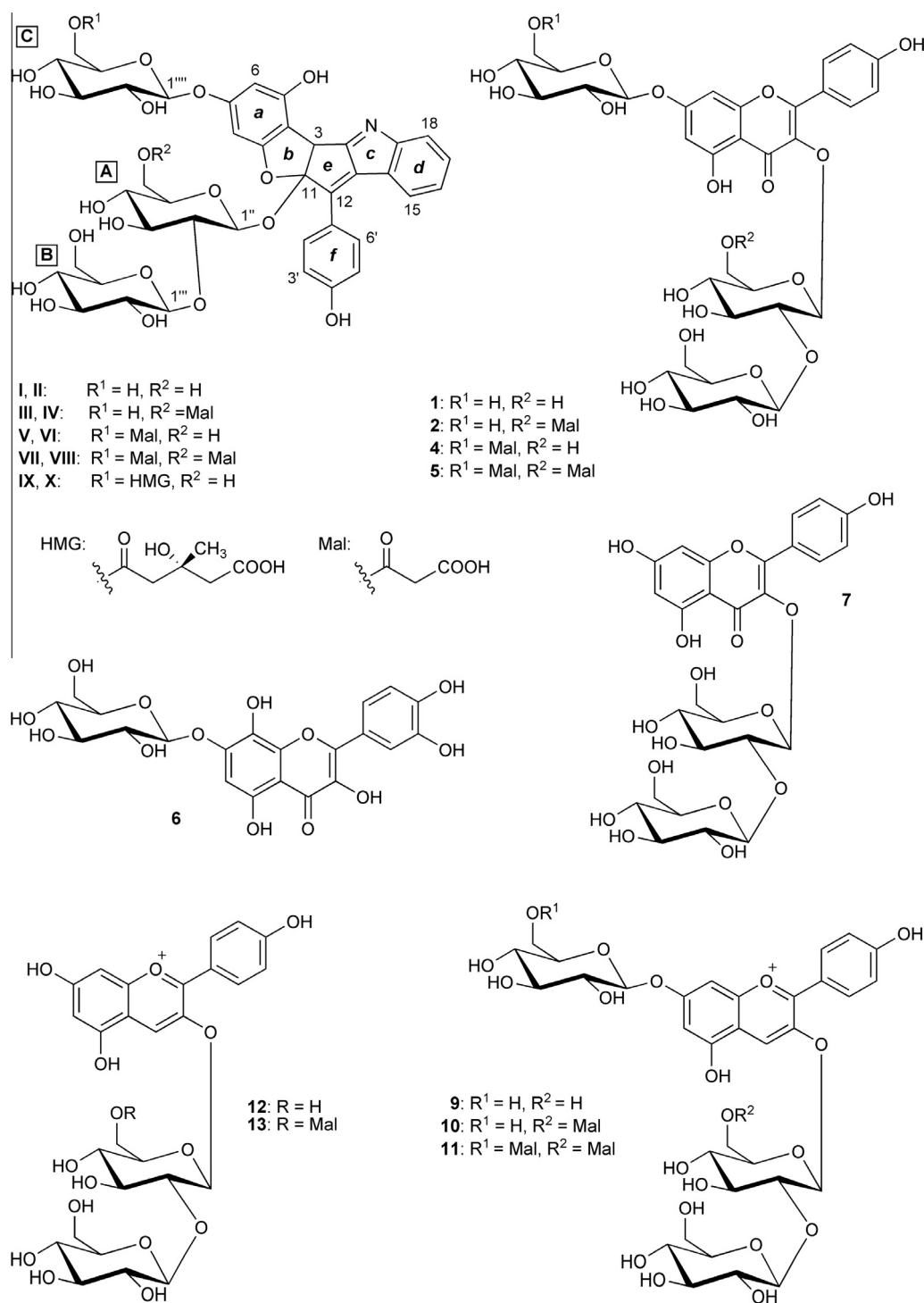
I, II:　　R¹ = H, R² = H
III, IV:　R¹ = H, R² =Mal
V, VI:　　R¹ = Mal, R² = H
VII, VIII:　R¹ = Mal, R² = Mal
IX, X:　　R¹ = HMG, R² = H

1: R¹ = H, R² = H
2: R¹ = H, R² = Mal
4: R¹ = Mal, R² = H
5: R¹ = Mal, R² = Mal

HMG:

Mal:

7

6

12: R = H
13: R = Mal

9: R¹ = H, R² = H
10: R¹ = H, R² = Mal
11: R¹ = Mal, R² = Mal

Fig. 2. Structures of the major pigments of petals from *P. nudicaule*, *P. alpinum* and *M. cambrica*, respectively. **I–X**: nudicaulins; **1, 2, 4–7**: flavonols, **3** and **8** (not shown) are isomers of **5** and **7**; **9–13**: anthocyanins.

the nudicaulin diastereomers **I** and **II**. A sample of nudicaulin **I** was used as a reference standard to establish a calibration curve (Fig. S5); this curve was used to quantify nudicaulins in petal extracts by HPLC at 460 nm. The results (Table 1) showed that the concentration of nudicaulins in the yellow flowers of *P. nudicaule* almost equals the concentration of nudicaulins in *M. cambrica*. It can also be seen that the concentration in the petals of *P. nudicaule* is higher than that in the petals of *P. alpinum*. In both *P. nudicaule* and *P. alpinum*, the nudicaulin content is lower in orange flowers than in yellow ones. Interestingly, in all the extracts, the concen-

tration of nudicaulin **I** is higher than that of its diastereomer, nudicaulin **II**.

3. Discussion

The species investigated here belong to different taxonomical units, and their habitats are scattered over the world. As mentioned above, *P. nudicaule* (Iceland poppy) and *P. alpinum* (alpine poppy) are members of the section *Meconella* that is distributed
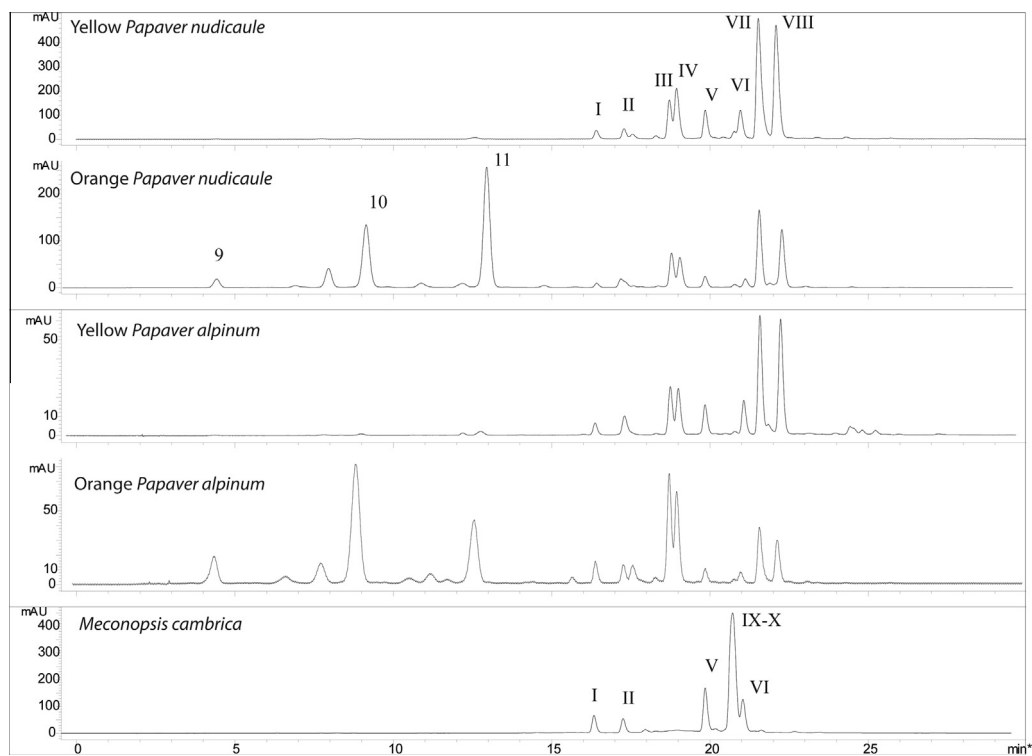
Fig. 3. HPLC profiles (method 2) detected at 460 nm from extracts of yellow petals of *P. nudicaule*, *P. alpinum* and *M. cambrica*, and of orange petals from *P. nudicaule* and *P. alpinum*. Peak labels correspond to the numbers assigned to compounds in Fig. 2.

in arctic-alpine areas (Carolan et al., 2006). Both species share many characteristics and, notably in wild populations, appear in dimorphic populations of white and yellow flowers (Elven et al., 2009), while garden varieties include orange flowering plants. In the case of *P. nudicaule*, genotypes with red petals are also known to occur (Table 1). Wind et al. (1998) studied the flower color dimorphism of *Papaver radicatum*, another arctic-alpine poppy, in its habitat. An altitude-dependent gradient was observed, according to which yellow flowers were more common in high altitudes while white flowering plants were more common in lower levels, close to the sea.

Papaver californicum, representing its own section (Kadereit, 1997), and *Papaver aculeatum*, a member of the section *Horrida* El-kan, may be similar to each other. The first species is indigenous to western North America, the second to South Africa. In contrast, *Papaver pilosum*, section *Pilosa* Prantl, and *Papaver atlanticum*, section *Pseudopilosa* M. Popov ex Günther, in southwestern Asia and North Africa, respectively, occur within areas typical of the genus *Papaver*. The opium poppy, *Papaver somniferum*, section *Papaver* L., is widespread as a crop plant (Kadereit, 1997; Carolan et al., 2006). Apart from *P. somniferum* var. *album*, the five species mentioned in this paragraph have orange or reddish petals (Table 1). In principle these characteristics do not exclude the presence of nudicaulins that is apparent in orange flowering *P. nudicaule* and *P. alpinum* plants.

M. cambrica (Welsh poppy) is the only European representative of a relatively large genus in the family of Papaveraceae that is also distributed in the Himalayans (Valtuena et al., 2012). Whereas this species has yellow flowers, other members of the genus have blue petals that are colored by anthocyanins and flavonols (Tanaka et al., 2001).

Often the color intensity (absorption) of flowers is enhanced by intermolecular co-pigmentation, e.g. different flavonoids (Goto and Kondo, 1991; Ono et al., 2010). However, the intense yellow color in flowers of *P. nudicaule* is conferred solely by the presence of

nudicaulins. The white color results from the absence of these compounds despite the presence of flavonols. The pelargonidin derivatives are responsible for red petals and the orange color is based on the co-occurrence of anthocyanins and nudicaulins. We conclude that the pigmentome of *P. nudicaule* flowers is directly associated with the optical outcome. Corresponding considerations apply to the findings with *P. alpinum* petals. In the petals of *M. cambrica*, no significant amount of other pigments accompanied the nudicaulins. These characteristic compounds were localized only in the petals of the respective species and were not found in green and underground parts of the plants.

The clear result, namely that nudicaulins occur in *Meconella* species and in *M. cambrica* but are lacking in all other examined *Papaver* species of different sections, may indicate nudicaulin-containing species are outsiders within their genera. However, the conclusion does not suggest that *M. cambrica* has a close relationship to *P. somniferum*, *P. pilosum* and *P. atlanticum* as postulated by Carolan et al. (2006). The significance of nudicaulins for the position of *M. cambrica* in its genus (Kadereit et al., 2011) and to the relation between the section *Meconella* and the Asian *Meconopsis* would be established by the analysis of petals from yellow flowering Himalayan species.

As the nudicaulins from *M. cambrica* confirm, these compounds occur as diastereomeric pairs. The nudicaulin spectrum of the *Papaver* species differs from that of *M. cambrica* by the absence of nudicaulins **III** and **IV** as well as of **VII** and **VIII**. However, the pair **IX** and **X** occurs; this pair is monoacylated with HMG in the same position where the malonyl unit is attached in nudicaulins **V** and **VI** (Fig. 2). Diacylated nudicaulins are obviously not synthesized in *M. cambrica*.

The quantification of nudicaulins **I** and **II**, which represent the simplest diastereomeric pair, and of the new nudicaulins **IX** and **X** from *M. cambrica*, shows that the (3S,11R)-diastereomer and the (3R,11S)-diastereomer are present in a ratio different from 1:1. The unbalanced proportion of approximately 1.2:1 suggests the

Table 2
^{1}H and ^{13}C NMR spectroscopic data (500 MHz for ^{1}H; 125 MHz for ^{13}C; CD₃OD) of nudicaulins **IX** and **X**.[a]

No	Nudicaulin **IX**[b]		Nudicaulin **X**[b]	
	[1]H	[13]C	[1]H	[13]C
	δ, mult., J (Hz)	δ	δ, mult., J (Hz)	δ
Aglycon				
2		177.9		178.0
3	5.63, s	49.6	5.80, s	49.8
4		102.3		102.3
5		156.4		156.5
6	6.31, d, 1.8	99.4	6.31, d, 1.8	99.8
7		162.4		162.6
8	6.25, d, 1.8	92.2	6.25, d, 1.8	92.9
9		161.2		161.5
11		126.0		125.7
12		169.7		169.7
13		131.6		131.6
14		122.9		123.2
15	8.31, d 7.8	125.7	8.31, d, 7.8	125.7
16	7.57, dd, 7.8, 7.8	128.6	7.57, dd, 7.8, 7.8	128.6
17	7.64, dd, 7.8, 7.8	131.5	7.64, dd, 7.8, 7.8	131.5
18	7.71, d, 7.8	117.4	7.71, d, 7.8	117.4
19		148.8		148.9
1′		123.1		123.1
2′/6′	8.62, d, 9.0	139.4	8.57, d, 9.0	139.6
3′/5′	7.14, d, 9.0	118.4	7.14, d, 9.0	118.4
4′		168.1		168.3
Glucose A[c]				
1″	4.80, d, 7.1	99.7	5.09, d, 7.9	97.6
2″	3.57	83.8	3.83	78.2
3″	3.55	77.5	3.67	78.9
4″	3.05	71.6	3.37	70.5
5″	3.24	75.9	3.39	77.7
6″A	3.80	62.1	3.68	61.7
6″B	3.72		3.63	
Glucose B[c]				
1‴	4.51, d, 7.7	106.3	4.95, d, 7.8	103.3
2‴	3.26	77.5	≈3.4	77.9
3‴	3.08	78.3	≈3.2	≈72
4‴	3.03	71.6	≈3.3	≈74
5‴	≈3.3	77.8	≈3.3	≈78
6‴A	3.31	62.7	3.70	63.1
6‴B	3.00		3.24	
Glucose C[c]				
1⁗	4.80, d, 7.0	102.1	4.82, d, 7.0	102.3
2⁗	3.37	77.1	3.39	74.4
3⁗	≈3.3	≈78	≈3.2	≈71
4⁗	3.40	≈74	3.40	≈74
5⁗	3.59	75.1	3.59	75.3
6⁗A	4.44, dd, 12.0, 2.1	64.1	4.42, dd, 12.0, 2.1	64.3
6⁗B	4.22, dd, 12.1, 5.8		4.20, dd, 12.0, 5.4	
3-Hydroxy-3-methyl-glutaryl				
1‴‴		172.4		172.3
2‴‴A	2.53, d, 15.3	46.4	2.62, d, 15.3	46.4
2‴‴B	2.48, d, 15.3		2.57, d, 15.3	
3‴‴		70.8		70.8
CH₃[a]	1.21, s	27.8	1.28, s	27.7
4‴‴A	2.64, d, 14.5	45.6	2.72, d, 14.5	45.8
4‴‴B	2.57, d, 14.5		2.66, d, 14.5	
5‴‴		174.9		175.0

[a] Some chemical shifts were obtained from 2D NMR spectra (COSY, TOCSY, HSQC, HMBC).
[b] Chemical shifts were obtained from a mixture of nudicaulins **IX** and **X** and may be interchanged between the two diastereomers.
[c] ^{1}H NMR signals of H-2–H-5 of glucose A, glucose B and glucose C partly overlap. Coupling constants were not determined.

preferred formation of the energetically favored (3*S*,11*R*)-diastereomer. The presence of scalemic mixtures of diastereomers in nature has been reported (Finefield et al., 2012). The occurrence of diastereomeric nudicaulins suggests it will be fruitful to investigate the mechanism underlying their formation in plant tissue.

4. Experimental

4.1. General experimental procedures

Preparative HPLC (method 1) was performed on a Merck-Hitachi LiChrograph chromatography system (L-6200A gradient pump, L-4250 UV/Vis detector) using a Purospher STAR RP18ec column (5 μm, 250 × 10 mm) and a linear gradient MeOH–H₂O (0.1% trifluoroacetic acid (TFA)) from 20% to 50% MeCN in 30 min (flow rate 3.5 ml min⁻¹; UV detection 254 nm). Analytical HPLC was performed on an Agilent series HP1100 (binary pump G1312A; auto sampler G1313A; diode array detector G1315B, 200–700 nm) using a Purospher STAR RP18ec column (5 μm, 250 × 4 mm; injection volume 10–25 μl). The following solvent and gradient systems were used: method 2: solvent A, 1% aq. TFA; solvent B, 1% TFA in MeCN, linear gradient from 10% B to 25% B in 25 min and isocratic for 5 min, flow rate 1 ml min⁻¹. The compounds were detected at 350 and 460 nm.

The LC–DAD–SPE–NMR system consisted of an Agilent 1100 chromatography system (quaternary solvent delivery pump G1311A, autosampler G1313A; Agilent Technologies, Waldbronn, Germany), a J&M photodiode array detector (DAD, detection 200–700 nm; J&M Analytik AG, Aalen, Germany), a Spark Prospekt 2 solid-phase extraction (SPE) device (Spark Holland, Emmen, The Netherlands), and a Bruker Avance 500 NMR spectrometer (Bruker, Karlsruhe, Germany) equipped with a TCI CryoProbe (5 mm) and a CryoFIT™ insert (cell volume 30 ml). The chromatographic separation was carried out by the use of method 2. A make-up pump (Knauer, Berlin, Germany) was used to add water (2.5 ml min⁻¹) to the eluent after HPLC in order to reduce the eluotropic capacity. Every LC peak was cumulatively trapped three times on HySphere resin GP cartridges (10 × 2 mm, 10 μm) (Spark). After the cartridges were dried with nitrogen gas, the analytes were eluted with CD₃CN or CD₃OD and transferred through a capillary to the NMR flow cell. NMR operating frequencies were 500.13 MHz for ^{1}H and 125.75 MHz for [13]C. The LC–DAD–SPE–NMR system was controlled by Bruker software HyStar 3.2, and the NMR data were acquired and processed using Topspin 2.1. The residual ^{1}H and ^{13}C NMR signals of solvents were used as an internal standard (δ 3.30 for ^{1}H and δ 48.97 for ^{13}C in CD₃OD; δ 2.00 for ^{1}H in CD₃CN).

NMR spectra (^{1}H NMR, ^{13}C NMR, ^{1}H-^{1}H COSY, TOCSY, HSQC, HMBC) of isolated nudicaulins were acquired in 5 mm or 2.5 mm tubes using the Bruker Avance NMR spectrometer and a TCI cryoprobe (5 mm) as described above but without the CryoFIT™ insert. HSQC experiments were acquired with a spectral width of 6009 Hz in the F_2 (^{1}H) dimension and 22638 in the F_1 (^{13}C) and with an acquisition time of 0.09 s. The relaxation delay was 2 s, the data collection matrix was 1024 × 256, the t_1 dimension was zero-filled to 1 k real data points, and a π/2 square sine bell window was applied in both dimensions. HMBC experiments were acquired with a spectral width of 6009 Hz in the F_2 (^{1}H) dimension and 31443 in the F_1 (^{13}C) and with an acquisition time of 0.37 s. The long-range delay was optimized for a coupling constant of 10 Hz. The relaxation delay was 2 s, the data collection matrix was 4048 × 256, the t_1 dimension was zero-filled to 1 k data points and a π/2 square sine bell window was applied in both dimensions. ROESY spectra were acquired using a spectral width of 6009 Hz, an acquisition time of 0.17 s, relaxation delay of 2 s, mixing time of 1000 ms, and 24 transients (four dummy scans) for each of the 256 increments. The mixing time was optimized using the t1ir1d pulse program.

The LC–MS system consisted of an Ultimate 3000 series RSLC (Dionex, Germaring, Germany) liquid chromatography and an Orbitrap mass spectrometer (Thermo Fisher Scientific, Bremen, Germany). HPLC was performed using an Acclaim C18 Column

(150 × 2.1 mm, 2.2 μm, Dionex) at a constant flow rate of 300 μl min⁻¹ using a binary solvent system: solvent A, H_2O with 0.1% HCOOH and solvent B, MeCN with 0.1% HCOOH. The HPLC gradient system started with 2% B and linearly increased to 30% B in 10 min, then increased to 90% B in 14 min, held for 4 min and brought back to the 2% B initial condition before being held for 5 min to re-equilibrate the column before the next injection. Full-scan mass spectra were generated using 30,000 m/Δm resolving power, and for MS² (CID) experiments, the resolution power was set to 7500 m/Δm. The mass accuracy was better than 3 ppm for MS and MS² experiments. Aliquots with concentrations of 40 μg ml⁻¹ of metabolites were used for LC/MS analysis.

4.2. Plant material

Seeds of *P. nudicaule* L., *P. alpinum* L. (both garden varieties), *P. somniferum* L. var. *nigrum*, *P. somniferum* L. var. *album*, and *P. californicum* A. Gray were obtained from the Leibniz Institute of Plant Genetics and Crop Plant Research (Gatersleben, Germany), germinated and grown in soil in the greenhouse facilities of the Max Planck Institute for Chemical Ecology (Jena, Germany) where voucher specimens are lodged. The temperature was 20–24 °C during the day and 18–21 °C during the night. Relative air humidity was between 60% and 70%. The natural daily photoperiod was supported with 16 h illumination from Phillips Sun-T Agro 400 Na lights. Fresh petals of *M. cambrica* (L.) Vig. were obtained from the botanical garden of the Friedrich Schiller University Jena, Germany. Lyophilized petals of *P. atlanticum* (Ball) Coss., *P. pilosum* Sibth. and Sm., and *P. aculeatum* Thunb. were provided by Prof. Kadereit, Institute of Special Botany and Botanical Garden, Johannes Gutenberg University Mainz, Germany.

4.3. Extraction and sample preparation

Fresh petals of *P. nudicaule*, *P. alpinum*, *M. cambrica* and other *Papaver* species and varieties were harvested, lyophilized, ground and extracted with 90% MeOH (3 × 25 ml) in an ultrasonic bath. The combined extracts were partitioned against n-hexane (3 × 30 ml) and the aqueous phase was used as follows: samples for semipreparative and quantitative analytical HPLC were passed through a PTFE membrane filter (0.45 μm) prior to injection. Samples for basic hydrolysis, isolation of nudicaulins **I** and **II** from *P. nudicaule* and nudicaulins **IX** and **X** from *M. cambrica* were used as described below.

4.4. Basic hydrolysis of acylated nudicaulins and isolation of nudicaulins **I** and **II**

The aqueous phase remaining after defatting the petal extracts of *P. nudicaule* was loaded on SPE cartridges (LiChrolut C₁₈; 1 g) and eluted with water (fraction A1), 30% MeOH (fraction A2), and finally with MeOH (fraction A3). Fractions A1 and A3 were discarded, while the colored fraction A2 was dried and then reconstituted in phosphate buffer (10 mM, pH 5.6). The solution was loaded onto a strong cation exchange (SCX) SPE cartridge (1 g). The efflux (fraction B1) and the eluate with MeOH (6 ml) (B2) contained the kaempferol glycosides. The last elution step using a 1:1 (v:v) mixture of conc. aqueous solution of NH_3 in MeOH (6 ml) resulted in fraction B3, which contained nudicaulins **I–VIII**. For basic hydrolysis, the fraction was evaporated to dryness and reconstituted in 50% MeOH (4 ml) in a 5 ml volumetric flask. NaOH (1 M, 600 μl) was added, filled to a volume of 5 ml by the addition of distilled water, and stirred for 30 min at room temperature. The progress of hydrolysis was monitored by HPLC (method 2). The hydrolysis was stopped by the addition of glacial acetic acid (100 μl). Nudicaulins **I** and **II** were isolated by prep. HPLC (method 1) and fully

characterized by NMR and MS. The aqueous phases of defatted petal extracts of *P. alpinum* (containing nudicaulins **I–VIII**) and *M. cambrica* (containing nudicaulins **I**, **II**, **V**, **VI**, **IX**, and **X**) were treated in the same manner.

4.5. Identification of nudicaulins, flavonols and anthocyanins

Nudicaulins **IX** and **X** were isolated from the *M. cambrica* crude extract by prep. HPLC (method 1) and analyzed as a mixture by NMR (Table 2) and MS. Nudicaulins **III**, **IV** and **V** were isolated from the *P. nudicaule* crude extract by prep. HPLC (method 1) and also analyzed by NMR. Nudicaulins **V** and **VI** were identified in the *P. nudicaule* crude extract by LC–SPE–NMR with LC method 2. The trapped analytes were transferred by capillary to the NMR flow cell as described above and measured in CD₃CN or CD₃OD. The MS data of nudicaulins were acquired by LCMS analysis of extracts as described above. The identification of flavonols and anthocyanins was based on LCMS analysis.

4.6. Calibration curve and quantification of nudicaulins

A stock solution of nudicaulin **I** (5 mg in 20% aq. MeOH) was prepared in a 5 ml volumetric flask. The stock solution was probed for purity by HPLC at different wavelengths (210, 254, 280, 350, 460 nm), and a purity of 89.2% was calculated based on the absorption at 210 nm. Five calibration solutions were prepared from the stock solution by dilution with 20% aq. MeOH in a 5 ml volumetric flask. Final nudicaulin **I** concentrations were 0.09, 0.18, 0.23, 0.36 and 0.45 mg ml⁻¹. The calibration solutions were stored in a refrigerator (+4 °C) in tightly closed vials until use. A volume (10 μl) of each calibration solution was injected five times and measured by HPLC (method 2). A calibration curve was derived (Fig. S5). Each of the hydrolyzed nudicaulin samples obtained from petals was probed three times by HPLC (method 2) to investigate for the presence of nudicaulins.

4.7. Analytical data of nudicaulins

4.7.1. Nudicaulin **IX**
¹H NMR and ¹³C NMR data are shown in Table 2. HRESIMS: m/z 1016.30187 ([M+H]⁺, $C_{47}H_{54}NO_{24}$, calc. 1016.30358). ESIMS/MS: m/z 692 [M+H-2Glc]⁺ (rel. int. 100), 386 [M+H-3Glc-HMG]⁺ (58), 854 [M+H-Glc]⁺ (12).

4.7.2. Nudicaulin **X**
¹H NMR and ¹³C NMR data are shown in Table 2. HRESIMS: m/z 1016.30187 ([M+H]⁺, $C_{47}H_{54}NO_{24}$, calc. 1016.30358). ESIMS/MS: m/z 692 [M+H-2Glc]⁺ (rel. int. 100), 386 [M+H-3Glc-HMG]⁺ (58), 854 [M+H-Glc]⁺ (12).

Appendix A. Supplementary data

Supplementary data associated with this article can be found, in the online version, at http://dx.doi.org/10.1016/j.phytochem.2013.04.011.

References

Carolan, J.C., Hook, I.I., Chase, M.W., Kadereit, J.W., Hodkinson, T.R., 2006. Phylogenetics of *Papaver* and related genera based on DNA sequences from ITS nuclear ribosomal DNA and plastid trnL intron and trnL-F intergenetic spacers. Ann. Bot. 98, 141–155.

Cornuz, G., Wyler, H., Lauterwein, J., 1981. Pelargonidin 3-malonylsophoroside from the red Iceland poppy *Papaver nudicaule*. Phytochemistry 20, 1461–1462.

Elven, R., Petrovsky, V.V., Solstad, H., 2009. Typification of names in *Papaver* sect. *Meconella* Spach (Papaveraceae). Taxon 58, 985–990.

Fabergé, A.C., 1943. The genetics of the Scapiflora section of *Papaver*. II. The alpine poppy. J. Genet. 45, 139–170.

Finefield, J.M., Sherman, D.H., Kreitman, M., Williams, R.M., 2012. Enantiomeric natural products: occurrence and biogenesis. Angew. Chem. Int. Ed. Engl. 51, 4802–4836.

Goto, T., Kondo, T., 1991. Structure and molecular stacking of anthocyanins – flower color variation. Angew. Chem. Int. Ed. Engl. 30, 17–33.

Grotewold, E., 2006. The genetics and biochemistry of floral pigments. Annu. Rev. Plant Biol. 57, 761–780.

Harborne, J.B., 1965. Plant polyphenols. XV. Flavonols as yellow flower pigments. Phytochemistry 4, 647–657.

Kadereit, J.W., 1997. The genus *Papaver* L. in the Mediterranean area. Lagascalia 19, 83–92.

Kadereit, J.W., Preston, C.D., Valtuena, F., 2011. Is Welsh poppy, *Meconopsis cambrica* (L.) Vig. (Papaveraceae), truly a *Meconopsis*? New J. Bot. 1, 80–88.

Morikawa, T., Wang, L.B., Ninomiya, K., Nakamura, S., Matsuda, H., Muraoka, O., Wu, L.J., Yoshikawa, M., 2009. Medicinal flowers. XXX. Eight new glycosides, everlastosides F-M, from the flowers of *Helichrysum arenarium*. Chem. Pharm. Bull. 57, 853–859.

Ono, E., Ruike, M., Iwashita, T., Nomoto, K., Fukui, Y., 2010. Co-pigmentation and flavonoid glycosyltransferases in blue *Veronica persica* flowers. Phytochemistry 71, 726–735.

Price, J.R., Robinson, R., Scott-Moncrieff, R., 1939. The yellow pigment of *Papaver nudicaule* Part I. J. Chem. Soc., 1465–1468.

Schliemann, W., Schneider, B., Wray, V., Schmidt, J., Nimtz, M., Porzel, A., Böhm, H., 2006. Flavonols and an indole alkaloid skeleton bearing identical acylated glycosidic groups from yellow petals of *Papaver nudicaule*. Phytochemistry 67, 191–201.

Struijs, K., Vincken, J.-P., Verhoef, R., Voragen, A.G.J., Gruppen, H., 2008. Hydroxycinnamic acids are ester-linked directly to glucosyl moieties within the lignan macromolecule from flaxseed hulls. Phytochemistry 69, 1250–1260.

Tanaka, M., Fujimori, T., Uchida, I., Yamaguchi, S., Takeda, K., 2001. A malonylated anthocyanin and flavonols in blue *Meconopsis* flowers. Phytochemistry 56, 373–376.

Tanaka, Y., Sasaki, N., Ohmiya, A., 2008. Biosynthesis of plant pigments: anthocyanins, betalains and carotenoids. Plant J. 54, 733–749.

Tatsis, E.C., Schaumlöffel, A., Warskulat, A.C., Massiot, G., Schneider, B., Bringmann, G., 2013. Nudicaulins, yellow flower pigments of *Papaver nudicaule*: revised constitution and assignment of absolute configuration. Org. Lett. 15, 156–159.

Valtuena, F., Preston, C.D., Kadereit, J.W., 2012. Phylogeography of a tertiary relict plant, *Meconopsis cambrica* (Papaveraceae), implies the existence of northern refugia for a temperate herb. Mol. Ecol. 21, 1423–1437.

Wind, O., Christensen, S.B., Mølgaard, P., 1998. Colouring agents in yellow and white flowered *Papaver radicatum* in Northern Greenland. Biochem. Syst. Ecol. 26, 771–779.